

Time-lapse change in anisotropy in Japan's near surface after the 2011 Tohoku-Oki earthquake

Nori Nakata¹ and Roel Snieder¹

Received 11 April 2012; revised 9 May 2012; accepted 15 May 2012; published 14 June 2012.

[1] We apply seismic interferometry to strong-motion records to detect the near-surface (i.e., an upper few hundred meters deep) change in anisotropy caused by the M_W 9.0 Tohoku-Oki earthquake on 11 March 2011. We show that the earthquake increased the difference between fast and slow shear-wave velocities arising from shear-wave splitting in most parts of northeastern Japan, but it did not significantly change fast shear-wave polarization directions in the near surface. Through monitoring of anisotropy and shear-wave velocity, we find that the changes in anisotropy and velocity partially recover with time; they are, however, still different from the pre-event values after nine months. The comparison of the spatial distribution between changes in anisotropy and velocity indicates the changes in anisotropy and velocity are generally correlated, especially in the northeastern Honshu (the main island in Japan). The change in the largest principal stress direction weakly correlates with the change in anisotropy. **Citation:** Nakata, N., and R. Snieder (2012), Time-lapse change in anisotropy in Japan's near surface after the 2011 Tohoku-Oki earthquake, *Geophys. Res. Lett.*, *39*, L11313, doi:10.1029/2012GL051979.

1. Introduction

[2] The change in near-surface shear-wave velocity caused by the M_W 9.0 Tohoku-Oki earthquake on 11 March 2011 is documented by *Nakata and Snieder* [2011]. The earthquake, among the largest in recent history, resulted in a reduction in the near-surface velocity averaged over two months following the earthquake of about 5% throughout northeastern Japan (a region 1,200 km wide). In this study, we estimate the change in near-surface polarization anisotropy by applying seismic interferometry to seismograms recorded by KiK-net, a strong-motion recording network operated by the National Research Institute for Earth Science and Disaster Prevention (NIED).

[3] Conventionally, shear-wave splitting is estimated by the cross-correlation method [e.g., *Fukao*, 1984]. One can estimate the fast and slow shear-wave polarization directions and the delay time between the fast and slow shear waves, which are mean values along a ray path. Moreover, using a cluster of earthquakes, one can estimate the vertical variation of anisotropy [e.g., *Okada et al.*, 1995].

[4] Earlier studies indicated that both the polarization directions and the splitting time change after large earth-

quakes [e.g., *Tadokoro et al.*, 1999]. In contrast, quite a few studies report no clear temporal change following major earthquakes [e.g., *Cochran et al.*, 2003; *Peng and Ben-Zion*, 2005; *Cochran et al.*, 2006]. Other studies have found that the splitting time increases after intermediate or large earthquakes, but the polarization directions do not change [e.g., *Saiga et al.*, 2003; *Liu et al.*, 2004] because the splitting time is more sensitive to change in stress than the polarization direction is [*Peacock et al.*, 1988]. Since changes in splitting times have been observed prior to major earthquakes [e.g., *Peacock et al.*, 1988; *Crampin et al.*, 1990; *Crampin and Gao*, 2005], monitoring the splitting time has been proposed as a diagnostic for earthquake prediction [*Crampin et al.*, 1984b].

[5] We present the change in anisotropy based on shear-wave splitting caused by the Tohoku-Oki earthquake inferred from seismic interferometry. First, we show shear-wave splitting at one KiK-net station. Then we compute changes in polarization anisotropy after the main event for all available stations and compare with the changes in shear-wave velocity and the largest principal stress direction caused by the main shock.

2. Earthquake Records and the Analyzing Method

2.1. KiK-net

[6] KiK-net, which includes about 700 stations all over Japan, has recorded strong motions continuously since the end of the 1990s [*Okada et al.*, 2004]. Each KiK-net station has a borehole a few hundred meters deep and two three-component seismographs, with a 0.01-s sampling interval, at the top and bottom of the borehole. In this study, we use the stations which have the borehole sensor at a depth between 100–337 m, and 91% of the receivers are at a depth less than 210 m. All the earthquakes used here are at a depth greater than 7 km, which is large compared to the depth of the boreholes. The velocity in the near surface is much slower than at greater depths. Since we consider events much deeper than the borehole, and because of the slow velocities at the near surface, we assume the waves propagate from the borehole to the surface receivers as plane waves in the vertical direction at each station.

[7] To confirm this assumption, we compute the angle of incidence θ by employing the procedure proposed by *Nakata and Snieder* [2012] using ray tracing. All earthquake data used have $\cos \theta > 0.975$, which means the maximum of the estimated velocity bias is 2.5%. The bias is, in practice, much smaller because of the employed averaging over many earthquakes. This inaccuracy does not contribute to the estimated shear-wave splitting because $\cos \theta$ is the same for the waves in all polarization directions.

¹Center for Wave Phenomena, Department of Geophysics, Colorado School of Mines, Golden, Colorado, USA.

Corresponding author: N. Nakata, Center for Wave Phenomena, Department of Geophysics, Colorado School of Mines, 1500 Illinois St., Golden, CO 80401, USA. (nnakata@mines.edu)

2.2. Seismic Interferometry

[8] By applying deconvolution-based seismic interferometry to the seismograms of each station, in which we deconvolve the seismogram at a surface receiver with that at a borehole receiver, we retrieve the wave propagating from the borehole receiver to the surface receiver [Nakata and Snieder, 2011], and then we apply a bandpass filter from 1 to 13 Hz to the deconvolved waveforms. To estimate the fast and slow polarization directions resulting from shear-wave splitting, we follow the seismic-interferometry approach of Miyazawa *et al.* [2008]. First, we rotate the seismograms recorded at the surface and borehole sensors in 10-degree increments in polarization. We then deconvolve the waveforms for each polarization direction to extract the shear wave that propagates from the borehole receiver to the surface receiver. We chose to use an increment of 10 degrees because when we computed the shear-wave splitting for 10 stations with an increment of one degree, the estimated anisotropy was the same as we obtained using an increment of 10 degrees. Based on the travel times for the propagating waves, we calculate the shear-wave velocities in each polarization using the known depth of the borehole. To find the travel times, we pick the three adjacent samples that have the largest amplitude and interpolate using a quadratic function since the sampling interval is not small enough to estimate the changes in the travel time caused by an earthquake [Nakata and Snieder, 2012].

[9] Comparing the travel times as a function of polarization and interpolating the arrival time and the polarization direction using a quadratic function, we estimate the fast and slow shear-wave velocities and polarization directions at the near surface, and then separate the obtained shear-wave velocity into one velocity averaged over direction (i.e., isotropic velocity) and direction-dependent velocity (i.e., anisotropic velocity) using Fourier series [Nakata and Snieder, 2012].

[10] A part of the controversy that major earthquakes do or do not change anisotropy comes from the differences of ray paths of smaller earthquakes used for analyzing polarization anisotropy [Peng and Ben-Zion, 2005]. By applying seismic interferometry, we estimate the polarization direction and the strength of anisotropy averaged over a top few-hundred meter (very shallow zone compared to other studies) for the fixed vertical path between the borehole and surface sensors.

[11] The method proposed by Liu *et al.* [2004] can be also used to estimate the travel times of the fast and slow shear waves by using waves that reflect off the free surface and propagate back to the borehole receiver. However, because their method uses reflected waves recorded at the borehole sensor and computes the autocorrelation of the borehole record, one cannot eliminate the imprint of the power spectrum of the incoming wave; hence the autocorrelated waves can be contaminated by variations in the power spectrum of the incident waves. In contrast, our method uses the direct wave for the deconvolution, so that we can cancel the imprint of the incoming wave, thus allowing for more accurate measurements of the travel times of the fast and slow shear waves.

3. The Change in Anisotropy Caused by the Tohoku-Oki Earthquake

[12] We first present earthquake records of KiK-net station FKSH12, which is in the Fukushima prefecture (220 km

west-southwest from the main-shock epicenter: Figure S1 in the auxiliary material).¹ Earthquakes used here were recorded from 1 May 2010 to 31 December 2011, the magnitude range is confined from 3.0 to 9.0. We compute the isotropic shear-wave velocities and the anisotropy coefficients, $(v_{fast} - v_{slow}) / v_{fast}$ (where v_{fast} and v_{slow} are the fast and slow velocities, respectively), of each earthquake (Figure 1). Figure S2 illustrates time variations of the velocities and the anisotropy coefficients at stations IWTH03 and TYMH04 from 1 January 2011 to 26 May 2011.

[13] At the bottom of Figure 1, we show the mean values of isotropic shear-wave velocities and anisotropy coefficients during the periods of 1 May 2010–10 March 2011, 12 March 2011–26 May 2011, and 27 May 2011–31 December 2011. The range of each value is the 95% confidence interval of the mean, and it is different from the gray shaded areas in Figure 1. The gray shaded areas indicate the mean values \pm one standard deviation of individual measurements. Based on Student's *t*-test [e.g., Bulmer, 1979], the mean velocities and mean anisotropy coefficients are significantly different between each consecutive pair of periods (Probability > 99.7%). After the main shock, the shear-wave velocity decreases (6%) and the anisotropy coefficient increases (60%), and these changes partially recover with time (mean velocity: 770 \rightarrow 723 \rightarrow 743 m/s and mean anisotropy coefficient: 7.8 \rightarrow 12.5 \rightarrow 10.8%). Nakata and Snieder [2011] discuss the change in the shear-wave velocity caused by the Tohoku-Oki earthquake. Because the fluid condition in cracks is one major cause of anisotropy [Crampin *et al.*, 1984a], large and intermediate earthquakes, which induce a stress change to open or close cracks [Nur and Simmons, 1969] and extend cracks [Atkinson, 1984], can change the anisotropy coefficient.

[14] As shown by the moving average of the anisotropy coefficient (the blue line in Figure 1, bottom), the anisotropy coefficient continues to increase for more than one month after the main shock, which might be caused by several large aftershocks during that period; the gradual increase is, however, not statistically significant. In contrast, the velocity decreases suddenly at the time of the main shock (see the blue line in Figure 1, top).

[15] The moving average of the anisotropy coefficient decreases before the main shock (the blue line in Figure 1, bottom), but it is not as significant as the changes between each pair of periods. Although some studies report changes in anisotropy before large earthquakes [e.g., Crampin *et al.*, 1990; Crampin and Gao, 2005], we need to consider the influence of intermediate earthquakes that occur before the main shock; such events may change the anisotropy as well. For example, the M6.2 earthquake on 13 June 2010 (a distance of 100 km and a depth of 40 km from station FKSH12) and the M5.7 earthquake on 29 September 2010 (a distance of 40 km and a depth of 8 km from the station) might both have been sources of elevated the anisotropy coefficient. The absence of such intermediate events in the nine weeks before the main earthquake near the station could have caused the observed reduction of the anisotropy coefficient in that period.

[16] We estimate the fast polarization directions and the anisotropy coefficient for all available stations throughout

¹Auxiliary materials are available in the HTML. doi:10.1029/2012GL051979.

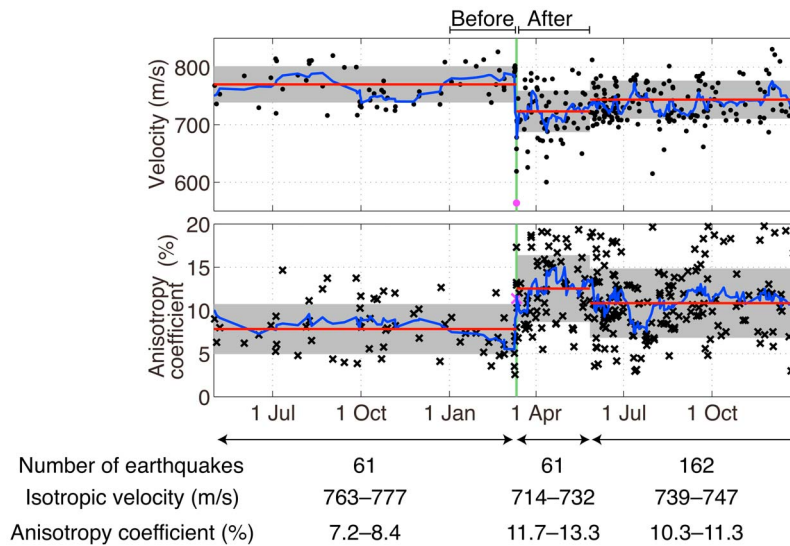


Figure 1. Variation in shear-wave velocity and anisotropy coefficient from 1 May 2010 to 31 December 2011 at station FKSH12. (top) The isotropic velocity of each earthquake (black dot) and its nine-point moving average (blue line). (bottom) The anisotropy coefficient computed from fast and slow shear-wave velocities (black cross) and its nine-point moving average (blue line). The velocity and the anisotropy coefficient estimated from the main event are illustrated by magenta symbols. Green vertical lines denote the origin time of the event. Red horizontal lines and gray shaded areas are the mean values and the mean values \pm the standard deviations of the measurements of all used earthquakes during each period. We show the number of earthquakes used and mean values of each period at the bottom. The range of each value is the 95% confidence interval of the mean. The bars at the top of the figure illustrate the time intervals used in Figure 2.

Japan for a period before the main earthquake (1 January 2011–10 March 2011) and a period afterward (12 March 2011–26 May 2011) (Figure 2a). To reduce uncertainty, we use only stations that have 1) more than three earthquake records during both time intervals, 2) travel times of interferometric waves greater than 0.1 s, 3) anisotropy coefficients greater than 1%, and 4) a standard deviation of velocity measurements smaller than 5%. The average change in the angles of the fast shear-wave polarization directions before and after the main event over all used stations is 17 degrees; this is close to the uncertainty, 15 degrees, computed from data over 11 years [Nakata and Snieder, 2012]. We conclude that the fast shear-wave polarization direction does not change significantly as a result of the main shock.

[17] In contrast, the anisotropy coefficient in most parts of northeastern Japan increases after the earthquake. To evaluate the change in the anisotropy coefficient caused by the event, we define the change in anisotropy as $(AC_{after} - AC_{before})/AC_{before}$, where AC_{before} and AC_{after} are the anisotropy coefficients before and after the main shock, respectively. The change in the anisotropy coefficient is shown in the second map from the right in Figure 2a. In Figure 2b, we show a crossplot of the changes in the shear-wave velocity and the anisotropy coefficient in four regions defined by the small map in Figure 2a. The changes are reasonably well correlated in region II and poorly correlated in region I. Different from other regions, most measurements in region IV are in the lower-right quadrant where the velocity increases and the anisotropy coefficient decreases. Region IV is on the west side of the tectonic lines (the Median Tectonic Line and the Itoigawa-Shizuoka Tectonic Line: the black dashed lines in Figure 2a), and the geologic

age and the geomorphological classification both differ across these lines; the west side is an older mountain area and the east side consists of younger volcanics and sediments [Wakamatsu *et al.*, 2006].

4. Comparing the Changes in Anisotropy and Static Stress

[18] Changes in stress caused by intermediate and large earthquakes have been studied for decades [e.g., Hanks, 1977; King *et al.*, 1994; Baltay *et al.*, 2010]. The Tohoku-Oki earthquake changed the stress and strain conditions [Hasegawa *et al.*, 2011]. Changes in stress and strain induce changes in local permeability and pore pressure [Koizumi *et al.*, 1996], and thereby changes in the anisotropy coefficient [Zatsepin and Crampin, 1997]. Fluid-filled microcracks, which cause shear-wave splitting [Zatsepin and Crampin, 1997], usually align with the direction of *in situ* stress [Crampin, 1978]. Saiga *et al.* [2003] compare at two stations the time delays associated with shear-wave splitting with the change in the Coulomb stress, which is an indicator of how close a fault is to failure [e.g., King *et al.*, 1994]. Toda *et al.* [2011] and Yoshida *et al.* [2012] compute the change in stress in northeastern Japan caused by the Tohoku-Oki earthquake.

[19] We compare the change in the anisotropy coefficient with the change in the largest principal stress direction computed by Yoshida *et al.* [2012] who used the damped stress tensor inversion method (Figure 3). We use this change as a proxy for changes in the stress. Since we do not know how the change in principal stress direction is related to the orientation of microfractures, which may either close or open in response to the change in stress, we cannot

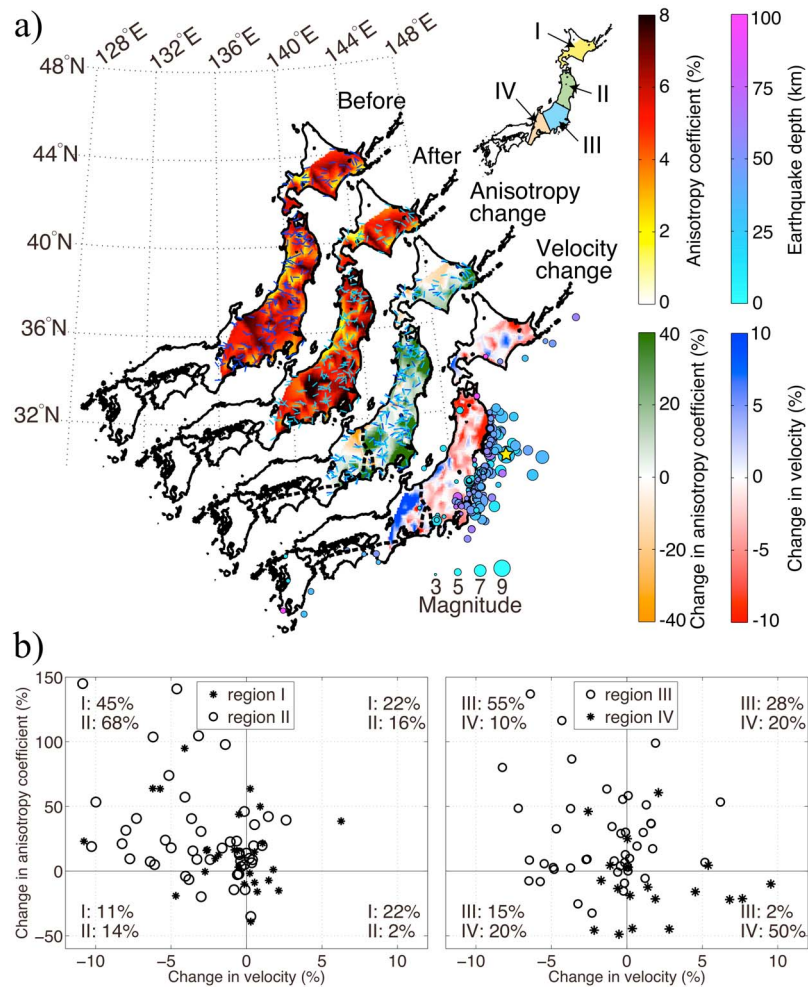


Figure 2. (a) Changes in shear-wave velocity and anisotropy coefficient after the Tohoku-Oki earthquake. Each map has a label at upper-right: anisotropy coefficients before (Before: 1 January 2011 to 10 March 2011) and after (After: 12 March 2011 to 26 May 2011) the Tohoku-Oki earthquake, its change, defined as $(AC_{after} - AC_{before})/AC_{before}$ (Anisotropy change), and the change in the isotropic shear-wave velocity (Velocity change). Dark blue (before) and light blue (after) arrows on the Before, After, and Anisotropy-change maps represent the direction of fast shear-wave polarization. We plot polarization-direction arrows without the change in the anisotropy coefficient in Figure S3. The longitude and latitude pertain to the leftmost map. The dashed black lines show the locations of major tectonic lines (the Median Tectonic Line and the Itoigawa-Shizuoka Tectonic Line) [Ito *et al.*, 1996]. Locations and magnitude of the earthquakes from 1 January 2011 to 26 May 2011 are shown as circles and relative to the rightmost map. The size of each circle indicates the magnitude of each earthquake and the color represents its depth. The yellow star denotes the epicenter of the Tohoku-Oki earthquake. The small Japanese map at the top shows four regions for interpretation in Figure 2b. (b) Crossplot of the changes in shear-wave velocity and anisotropy coefficient in the regions. Each symbol indicates the data of each station. The numbers in the corners of each panel show the fraction of stations in each quadrant of all stations in each region.

compute the change in anisotropy because of the change in stress. In Figure 3b, the changes in the largest principal stress direction and the anisotropy coefficient, which are both averaged over a 0.5° grid, indicate a weak positive correlation except for areas B, J, K, and L. A large change in the principal stress direction ($>20^\circ$) signifies that the stress condition before and after the main shock is significantly different; therefore a large change in the principal stress direction might induce the large change in the anisotropy coefficient ($> \pm 10\%$) in areas A, C, and G (the blue circle in Figure 3b). Likewise, a small change in the principal stress direction ($<20^\circ$) is coincident with the small change in the

anisotropy coefficient ($< \pm 10\%$) in areas D, E, F, H, I, and M (the red circle in Figure 3b).

[20] Areas J and K (the asterisks in Figure 3b) are on the west side of the tectonic lines and area L is close to these lines, and the change in stress caused by the main event in the upper few hundred meters (the depth range of the boreholes) might be different on both sides of the tectonic lines. Kern [1978] found in rock-physics experiments that as the confining pressure increases, velocity increases and anisotropy decreases. We speculate that the increase in the velocity and the decrease in the anisotropy coefficient on the west side of the tectonic lines could be explained by increase in the compressional stress, but since we cannot directly measure

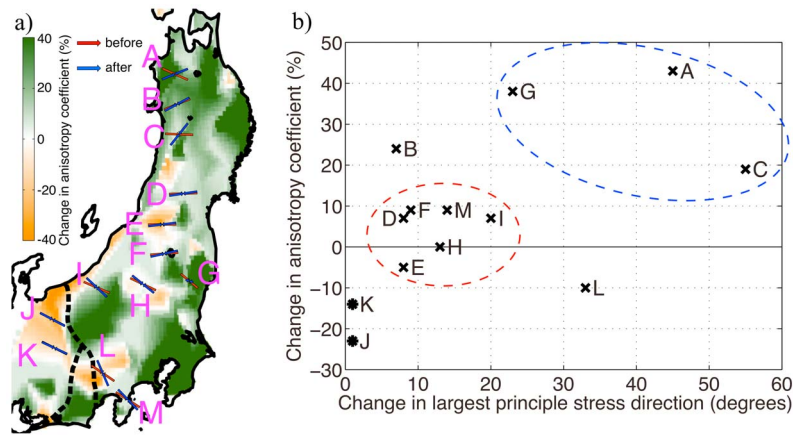


Figure 3. (a) Anisotropy change in Figure 2a with the largest principal stress direction [from Yoshida *et al.*, 2012, Figure 3], before (red arrows) and after (blue arrows) the Tohoku-Oki earthquake. The arrows are estimated in each 0.5° -grid area. Black dashed lines indicate the locations of the major tectonic lines. A-M areas denote the interpreted regions in Figure 3b as well as Yoshida *et al.* [2012]. (b) Crossplot of the changes in the largest principal stress direction [Yoshida *et al.*, 2012] and the anisotropy coefficient in each area shown in Figure 3a. The change in the anisotropy coefficient is the mean value for each 0.5° grid. Asterisk indicate the areas on the west side of the tectonic lines. The blue and red dashed circles indicate two groups which have a correlation between the changes in the largest principle stress direction and in the anisotropy coefficient.

the compressional stress in this study, we cannot validate this hypothesis. Note that the model of Yoshida *et al.* [2012] does not include possible differences in compaction and in rheology across these lines. The change in the principal stress direction is only one proxy of changes in stress, and we cannot explain the change in the anisotropy coefficient in area B from the change in the principal stress direction.

5. Conclusion

[21] By applying deconvolution-based seismic interferometry to KiK-net data, we measure changes in anisotropy caused by the Tohoku-Oki earthquake. The anisotropy coefficient increases in most parts of northeastern Japan after the Tohoku-Oki earthquake, but the fast polarization direction does not significantly change. The changes in shear-wave velocity and anisotropy both partly recover with time. Comparison of the changes in the shear-wave velocity and the anisotropy coefficient shows strong correlation in the northeastern half of Honshu. Also, the changes in the anisotropy coefficient and the largest principal stress direction are weakly correlated. On the west side of the tectonic lines, the increase in velocity and the decrease in anisotropy could be explained by a difference of the change in stress across the tectonic lines.

[22] **Acknowledgments.** We are grateful to NIED for providing us with the KiK-net data. We thank Ken Lamer, Elizabeth Cochran, Michael Wyssession, and an anonymous reviewer for valuable suggestions, correlations, edits, and discussions.

[23] The Editor thanks Elizabeth Cochran and an anonymous reviewer for assisting in the evaluation of this paper.

References

Atkinson, B. K. (1984), Subcritical crack growth in geological materials, *J. Geophys. Res.*, *89*(B6), 4077–4114.
 Baltay, A., G. Prieto, and G. C. Beroza (2010), Radiated seismic energy from coda measurements and no scaling in apparent stress with seismic moment, *J. Geophys. Res.*, *115*, B08314, doi:10.1029/2009JB006736.
 Bulmer, M. G. (1979), *Principles of Statistics*, Dover, New York.

Cochran, E. S., J. E. Vidale, and Y.-G. Li (2003), Near-fault anisotropy following the Hector Mine earthquake, *J. Geophys. Res.*, *108*(B9), 2436, doi:10.1029/2002JB002352.
 Cochran, E. S., Y.-G. Li, and J. E. Vidale (2006), Anisotropy in the shallow crust observed around the San Andreas fault before and after the 2004 M 6.0 Parkfield earthquake, *Bull. Seismol. Soc. Am.*, *96*(4B), S364–S375.
 Crampin, S. (1978), Seismic-wave propagation through a cracked solid: Polarization as a possible dilatancy diagnostic, *Geophys. J. R. Astron. Soc.*, *53*, 467–496.
 Crampin, S., and Y. Gao (2005), Comment on “Systematic analysis of shear-wave splitting in the aftershock zone of the 1999 Chi-Chi, Taiwan, earthquake: Shallow crustal anisotropy and lack of precursory changes, by Yungfeng Liu, Ta-Liang Teng, and Yehuda Ben-Zion,” *Bull. Seismol. Soc. Am.*, *95*, 354–360.
 Crampin, S., E. M. Chesnokov, and R. G. Hipkin (1984a), Seismic anisotropy—The state of the art: II, *Geophys. J. R. Astron. Soc.*, *76*, 1–16.
 Crampin, S., R. Evans, and B. K. Atkinson (1984b), Earthquake prediction: A new physical basis, *Geophys. J. R. Astron. Soc.*, *76*, 147–156.
 Crampin, S., D. C. Booth, R. Evans, S. Peacock, and J. B. Fletcher (1990), Changes in Shear wave splitting at Anza near the time of the North Palm Springs earthquake, *J. Geophys. Res.*, *95*(B7), 11,197–11,212.
 Fukao, Y. (1984), Evidence from core-reflected shear waves for anisotropy in the Earth’s mantle, *Nature*, *309*, 695–698.
 Hanks, T. C. (1977), Earthquakes stress drops, ambient tectonic stresses and stresses that drive plate motions, *Pure Appl. Geophys.*, *115*, 441–458.
 Hasegawa, A., K. Yoshida, and T. Okada (2011), Nearly complete stress drop in the 2011 M_w 9.0 off the Pacific coast of Tohoku earthquake, *Earth Planets Space*, *63*, 703–707.
 Ito, T., T. Ikawa, S. Yamakita, and T. Maeda (1996), Gently north-dipping Median Tectonic Line (MTL) revealed by recent seismic reflection studies, southwest Japan, *Tectonophysics*, *264*, 51–63.
 Kern, H. (1978), The effect of high temperature and high confining pressure on compressional wave velocities in quartz-bearing and quartz-free igneous and metamorphic rocks, *Tectonophysics*, *44*, 185–203.
 King, G. C. P., R. S. Stein, and J. Lin (1994), Static stress changes and the triggering of earthquakes, *Bull. Seismol. Soc. Am.*, *84*(3), 935–953.
 Koizumi, N., Y. Kano, Y. Kitagawa, T. Sato, M. Takahashi, S. Nishimura, and R. Nishida (1996), Groundwater anomalies associated with the 1995 Hyogo-ken Nanbu earthquake, *J. Phys. Earth*, *44*, 373–380.
 Liu, Y., T.-L. Teng, and Y. Ben-Zion (2004), Systematic analysis of shear-wave splitting in the aftershock zone of the 1999 Chi-Chi, Taiwan, earthquake: Shallow crustal anisotropy and lack of precursory variations, *Bull. Seismol. Soc. Am.*, *94*(6), 2330–2347.
 Miyazawa, M., R. Snieder, and A. Venkataraman (2008), Application of seismic interferometry to extract P- and S-wave propagation and observation of shear-wave splitting from noise data at Cold Lake, Alberta, Canada, *Geophysics*, *73*(4), D35–D40.

- Nakata, N., and R. Snieder (2011), Near-surface weakening in Japan after the 2011 Tohoku-Oki earthquake, *Geophys. Res. Lett.*, *38*, L17302, doi:10.1029/2011GL048800.
- Nakata, N., and R. Snieder (2012), Estimating near-surface shear wave velocities in Japan by applying seismic interferometry to KiK-net data, *J. Geophys. Res.*, *117*, B01308, doi:10.1029/2011JB008595.
- Nur, A., and G. Simmons (1969), Stress-induced velocity anisotropy in rock: An experimental study, *J. Geophys. Res.*, *74*(27), 6667–6674.
- Okada, T., T. Matsuzawa, and A. Hasegawa (1995), Shear-wave polarization anisotropy beneath the north-eastern part of Honshu, Japan, *Geophys. J. Int.*, *123*, 781–797.
- Okada, Y., K. Kasahara, S. Hori, K. Obara, S. Sekiguchi, H. Fujiwara, and A. Yamamoto (2004), Recent progress of seismic observation networks in Japan—Hi-net, F-net, K-NET and KiK-net, *Earth Planets Space*, *56*, 15–28.
- Peacock, S., S. Crampin, D. C. Booth, and J. B. Fletcher (1988), Shear wave splitting in the Anza seismic gap, Southern California: Temporal variations as possible precursors, *J. Geophys. Res.*, *93*(B4), 3339–3356.
- Peng, Z., and Y. Ben-Zion (2005), Spatiotemporal variations of crustal anisotropy from similar events in aftershocks of the 1999 M7.4 İzmit and M7.1 Düzce, Turkey, earthquake sequences, *Geophys. J. Int.*, *160*, 1027–1043.
- Saiga, A., Y. Hiramatsu, T. Ooida, and K. Yamaoka (2003), Spatial variation in the crustal anisotropy and its temporal variation associated with a moderate-sized earthquake in the Tokai region, central Japan, *Geophys. J. Int.*, *154*, 695–705.
- Tadokoro, K., M. Ando, and Y. Umeda (1999), S wave splitting in the after-shock region of the 1995 Hyogo-ken Nanbu earthquake, *J. Geophys. Res.*, *104*(B1), 981–991.
- Toda, S., R. S. Stein, and J. Lin (2011), Widespread seismicity excitation throughout central Japan following the 2011 M = 9.0 Tohoku earthquake and its interpretation by Coulomb stress transfer, *Geophys. Res. Lett.*, *38*, L00G03, doi:10.1029/2011GL047834.
- Wakamatsu, K., M. Matsuoka, and K. Hasegawa (2006), GIS-based nationwide hazard zoning using the Japan engineering geomorphologic classification map, *Proc. U. S. Natl. Conf. Earthquake Eng.*, *8*, 849.
- Yoshida, K., A. Hasegawa, T. Okada, T. Iinuma, Y. Ito, and Y. Asano (2012), Stress before and after the 2011 great Tohoku-oki earthquake and induced earthquakes in inland areas of eastern Japan, *Geophys. Res. Lett.*, *39*, L03302, doi:10.1029/2011GL049729.
- Zatsepin, S. V., and S. Crampin (1997), Modelling the compliance of crustal rock—I. Response of shear-wave splitting to differential stress, *Geophys. J. Int.*, *129*, 477–494.